Geoengineering's role in reducing future Antarctic mass loss is unclear

Mira Adhikari[1], Daniel F. Martin[2], Tamsin L. Edwards[1], Antony J. Payne[3], James F. O'Neill[4], Peter J. Irvine[5]

[1]Department of Geography, King's College London, London, UK
[2]Applied Numerical Algorithms Group, Lawrence Berkeley National Laboratory, Berkeley, CA, USA
[3]Department of Earth, Ocean and Ecological Sciences, University of Liverpool, Liverpool, UK
[4]University of Exeter, Centre for Geography and Environmental Sciences, Exeter, UK
[5]Earth Sciences, University College London, London WC1E 6BT, UK

Key Points:

- Idealised geoengineering is unable to prevent significant loss from Antarctica regardless of emissions pathway or year of implementation
- Geoengineering in 2050 under high emissions reduces sea level contribution compared to stabilisation but geoengineering in 2100 increases it
- Surface mass balance gains initially offset loss under stabilisation, but this may be negated in future by accelerating dynamic loss

Corresponding author: Mira Adhikari, mira.adhikari@kcl.ac.uk

Abstract

Using the BISICLES ice sheet model, we compare the Antarctic ice sheet's response over the 22nd century in a scenario where idealised large scale, instantaneous geoengineering is implemented in 2100 or 2050 (geoengineering), with scenarios where the climate forcing is held constant in the same year (stabilisation). Results are highly climate model dependent, with larger differences between models than between geoengineering and stabilisation scenarios, but show that geoengineering cannot prevent significant losses from Antarctica over the next two centuries. If implemented in 2050, sea level contributions under geoengineering are lower than under stabilisation scenarios. If implemented in 2100, under high emissions, geoengineering produces higher sea level than stabilisation scenarios, as increased surface mass balance in the warmer stabilisation scenarios offsets some of the dynamic losses. Despite this, dynamic losses appear to accelerate and may eventually negate this initial offset, indicating that beyond 2200, geoengineering could eventually be more effective.

Plain Language Summary

Sea level will keep rising well into the next century as oceans and ice sheets take decades to respond to atmospheric temperature changes, even if aggressive greenhouse gas reduction policies were immediately implemented. Consequently, geoengineering has been proposed as a more rapid measure. Geoengineering refers to the manipulation the climate system to lessen the impacts of human induced warming. We use an ice sheet model to predict Antarctica's response to geoengineering in 2200, as it is one of the most uncertain sea level contributors. We find that, although the results depend strongly on which climate model is used to drive the ice sheet model, geoengineering cannot prevent sea level contribution from Antarctica. However, implementing geoengineering in 2050 produces smaller sea level rises compared with a scenario where the climate is stabilised in the same year. If geoengineering is delayed to 2100, sea level rise is worse under geoengineering, because stabilising the climate in 2100 creates a warmer climate where the air can hold more moisture, increasing snowfall on Antarctica and offsetting some mass loss. However, stabilising the climate also produces progressively bigger increases in ice discharge compared with geoengineering. This suggests that geoengineering may be more effective in future.

1 Introduction

The Antarctic ice sheet is the largest ice mass on the planet, containing the equivalent of 58m of sea level rise (Morlighem et al., 2020). It is also the most uncertain sea level contributor. Projected sea level contributions for Antarctica from the IPCC Sixth Assessment Report are 0.03-0.27m to 0.03-0.34m for 2100 for the low and high emission scenarios (SSPs: Shared Socioeconomic Pathways) SSP1-2.6 and SSP5-8.5, respectively (IPCC, 2021). Beyond 2100, projections for the ice sheet become even more uncertain, in part due to a relative lack of projections, but also due to remaining uncertainties in ice loss mechanisms, solid earth feedbacks, ice shelf rheology, and others (Bulthuis et al., 2019; Lowry et al., 2021).

An ice sheet's contribution to sea level is dictated by the difference between its surface mass balance (SMB) and ice dynamics. Surface mass balance processes encompass all gains and losses on the ice sheet's surface, including snow deposition, surface melting, runoff, and evaporation, and are primarily controlled by atmospheric changes (Hanna et al., 2013). Ice dynamics refer to losses through the calving and melting of ice shelves into the ocean, and are driven by oceanic changes. The combination of SMB and ice discharge make up an ice sheet's total mass balance. A positive mass balance indicates a net gain in ice mass, while a negative value indicates net mass loss and therefore a contribution to sea level. Currently, mass loss is primarily driven by ocean interactions (Pattyn

& Morlighem, 2020). In particular, upwelling of circumpolar deep water (CDW), a water mass over 4°C warmer than the freezing point at the base of an ice shelf, is widely accepted as a key driver of current basal melting in the Amundsen Sea (Jacobs et al., 2011; Pritchard et al., 2012; Rignot & Jacobs, 2002). Understanding the impacts of future climate change is difficult as ocean and atmospheric warming can produce contrasting effects (Payne et al., 2021; Edwards et al., 2021). Ocean warming amplifies mass loss through increased ice discharge, and while atmospheric warming increases the moisture holding capabilities of the air, leading to more precipitation and mass gain, it can also increase ice discharge through melting and runoff, which can lead to ice shelf breakup (Kittel et al., 2020).

Even if stringent emissions reduction policies were immediately implemented, sea level rise is projected to continue beyond 2200 due to the delayed response of the oceans and cryosphere to atmospheric temperature changes (climate inertia (IPCC, 2021)). To try and ameliorate some of these lagged climate responses, geoengineering has been proposed as a more extreme measure. Geoengineering describes a deliberate modification of the climate system to help mitigate the impacts of anthropogenic warming (Lockley et al., 2020). Geoengineering methods are broadly comprised of two types; carbon dioxide removal (CDR) and solar radiation management (SRM). CDR removes carbon dioxide from the atmosphere and stores it in long term sinks, while SRM increase the earth's albedo (Irvine et al., 2018). While SRM does not target the source of anthropogenic warming, its impacts would be felt more rapidly than CDR methods.

Geoengineering experiments are essential for understanding whether Antarctic mass losses would be irreversible, and if implementation could prevent the crossing of critical thresholds such as the initiation of marine ice sheet instability (MISI). MISI refers to the mechanism by which marine ice sheets could rapidly retreat via a destabilising of their grounding lines (Weertman, 1974). It can only occur in marine ice sheets where the bedrock in the interior is more depressed than the coasts, resulting in a retrograde slope (Pattyn & Morlighem, 2020). If an ice shelf thins, its buttressing capabilities on the ice sheet are reduced, accelerating ice flow and causing grounding line retreat (Schoof, 2007). As ice flux is a function of ice thickness at the grounding line, the retreat of the grounding line to deeper portions of the bed leads to a higher ice flux (Weertman, 1974). This creates a positive feedback of mass loss which can only be stabilised when the bed slope reverses or buttressing increases (Weertman, 1974; Gudmundsson, 2013).

Few studies have been done regarding geoengineering's impact on Antarctic mass loss. Garbe et al. (2020) show with equilibrium experiments that regrowth of the Antarctic ice sheet is much slower than deterioration (i.e. hysteresis), suggesting slow implementation of CDR may be ineffective. DeConto and Pollard (2016) showed that for high emission scenarios, implementing CDR in 2500 could reduce the sea level contribution from Antarctica more effectively than a natural reduction of CO_2 begun in the same year, but sea level rise remained very high: at 9.55m and 4.7m for high and mid emissions scenarios, respectively, even after 5000 years. These experiments were limited in scope, however, with a very late drawdown of CO_2, no ocean cooling, and were driven by a model that includes a mechanism of sustained ice front retreat known as marine ice cliff instability (MICI) and thus loses ice more rapidly than other models (IPCC, 2021, 2019). Sutter et al. (2023) find that SRM cannot prevent a collapse of the West Antarctic Ice Sheet under a high emissions scenario due to committed warming in the Southern Ocean, but that under a mid emission scenario, if implemented by mid century, collapse could be prevented.

Under an earlier application of CDR, DeConto et al. (2021) still show sustained sea level contribution from Antarctica. They see a distinct increase in contribution between CDR deployment in 2060 and 2070, suggesting the existence of a critical threshold of ice sheet loss. The authors attribute this to marine ice instabilities being triggered

due to the deterioration of ice shelves that cannot recover, even with rapid CDR, due to the ocean's slow response time.

Here, we also perform idealised CO_2 drawdown experiments to mimic an instantaneous application of geoengineering, but using an ice sheet model that does not invoke MICI processes. We compare the Antarctic ice sheet's response to a scenario where idealised, large scale CDR is immediately implemented in either 2100 or 2050 by instantly returning the climate to present day forcing, with ones where the climate is held constant in the same year. In doing so, we aim to improve understanding of reversibility and long term commitments of mass loss from Antarctica.

2 Methods

2.1 The BISICLES ice sheet model

This study used the Berkeley Ice Sheet Initiative for Climate at Extreme Scales (BISICLES) (Cornford et al., 2013). This model was chosen due to its adaptive mesh refinement capabilities, allowing it to better capture ice dynamics around grounding lines and ice streams. Modelling ice sheets requires fine spatial resolution (<1km) for these processes, but as interior changes are slower and on larger spatial scales, they do not require such high resolution. By using adaptive mesh refinement, high resolution is only used where it is necessary, reducing computational costs and allowing more simulations. Here, we apply a finest spatial resolution of 1km, reducing down to 8km in the interior.

2.2 Forcing scenarios

This work is based on extending Antarctic projections from the Ice Sheet Model Intercomparison Project for CMIP6 (ISMIP6), which compared a range of stand-alone ice sheet models to provide the most up to date understanding of ice sheet response to the climate system for the Climate Model Intercomparison Project Phase 6 (CMIP6) (Nowicki et al., 2016; Seroussi et al., 2019; Payne et al., 2021; J. O'Neill et al., 2024). Five experiments (experiments 5-8 and B7) were chosen to extend beyond 2100 from O'Neill et al. (2024). Three experiments are high emission scenarios under RCP8.5, and use GCMs NorESM1-M (*NorESM1 8.5*), MIROC-ESM-CHEM (*MIROC 8.5*) and CCSM4 (*CCSM4 8.5*). The other two experiments are low emission scenarios forced by NorESM1-M under RCP2.6 (*NorESM1 2.6*) and CNRM-CM6-1 under SSP1-2.6 (*CNRM 1-2.6*). These GCMs were selected for ISMIP6 via a thorough analysis process (Barthel et al., 2020), based on their ability to simulate present day Antarctic climate, in addition to sampling a range of atmospheric and ocean forcings, and the availability of both RCP8.5 and RCP2.6. CNRM was selected due to availability only, to provide an additional low forcing scenario (Payne et al., 2021).

The ice sheet model experiments were driven by both atmospheric and ocean forcing, both of which were provided by ISMIP6 directly from GCM output. The atmospheric projections consist of yearly SMB and surface temperature anomalies relative to a reference period of January 1995 to December 2014. Oceanic projections consist of thermal forcing anomalies (calculated from temperature and salinity) relative to 1995-2014, which were then added to an observed climatology (1995-2017) in order to calculate basal melt rates using the ISMIP6 melt parameterization (Jourdain et al. (2020)).

Climate forcings were extended beyond 2100 to 2200 by either repeating the climate forcing between 2091-2100 (simulating a stabilisation scenario with no geoengineering), or instantly returning to present day forcing of 2015-2024 (simulating an instant, large scale geoengineering application scenario). A second set of scenarios was generated using the same method but extending the climate forcing from 2050, to understand the effects of an earlier geoengineering implementation. In this case, the repeated time pe-

riod for the stabilisation scenario was 2051-2060. We refer to these as the 2100/2050 stabilisation and geoengineering scenarios, respectively.

3 Results

3.1 Total sea level contribution

Figure 1 shows the projected Antarctic sea level contribution for all experiments. Total sea level contribution is the change in volume above flotation (VaF) for grounded ice, calculated by

$$V_{af} = \left(min((Z - S), 0) \times \frac{\rho_{ocean}}{\rho_{ice}} + H \right) dx\ dy$$

where Z is topography, S is sea level, $\rho_{ocean} = 1028$ kg m^{-3} and $\rho_{ice} = 910$ kg m^{-3} are the densities of ocean water and ice respectively, and H is ice thickness. Table B1 summarises the projected changes for key variables at 2200 relative to 2012 for all experiments.

Regardless of scenario, Antarctica will contribute considerably to sea level rise over the next two centuries: up to 172mm. There is no clear distinction between high and low emission scenarios, with a large range in sea level contributions between models for the same scenario, indicating that the results are highly model dependent (Figure 1). For instance, in the 2050 scenarios, *NorESM1 2.6* stabilisation has a sea level contribution almost 70mm higher than *CCSM4 8.5* stabilisation.

Under RCP2.6/SSP1-2.6, geoengineering results in marginally lower sea level contributions than stabilisation for both 2050 and 2100 implementation. The difference in sea level contribution between the models' geoengineering and stabilisation scenarios (G-S difference) is smaller for the 2100 scenarios (<1-4mm) than the 2050 scenarios (3-11mm, B1).

The 2050 RCP8.5 scenarios show that, with the exception of *CCSM4 8.5*, geoengineering would result in a smaller sea level contribution than stabilisation. For *CCSM4 8.5*, geoengineering increases sea level by 2200, though the trajectory indicates that there may be recovery in future decades (Figures 1 and B1). G-S differences are higher than for low emissions, between 14-24mm (Figure B1).

The 2100 RCP8.5 emission experiments have more disagreement between models on the effectiveness of geoengineering. Geoengineering has a higher sea level contribution than stabilisation for *NorESM1 8.5* and *CCSM4 8.5* by 2200. However, both geoengineering trajectories appear to slow, while the stabilisation scenarios accelerate, suggesting that post 2200, geoengineering could eventually be more effective, with their G-S differences peaking and beginning to decrease (Figure B1). *MIROC 8.5* also initially shows a higher sea level contribution under geoengineering, but this reverses in ∼2185. *CCSM4 8.5* has a much larger G-S difference than the other two models.

In the following two sections, the two components that make up total sea level contribution (SMB and ice dynamics) are discussed.

3.2 Surface Mass Balance

Table B1 shows the integrated SMB sea level contribution in 2200. Values are negative as the data is shown in terms of sea level contribution. As with total sea level contribution, there is overlap between RCP8.5 and RCP2.6/SSP1-2.6 scenarios and a large spread in model projections. *NorESM1* consistently shows the weakest increases in SMB.

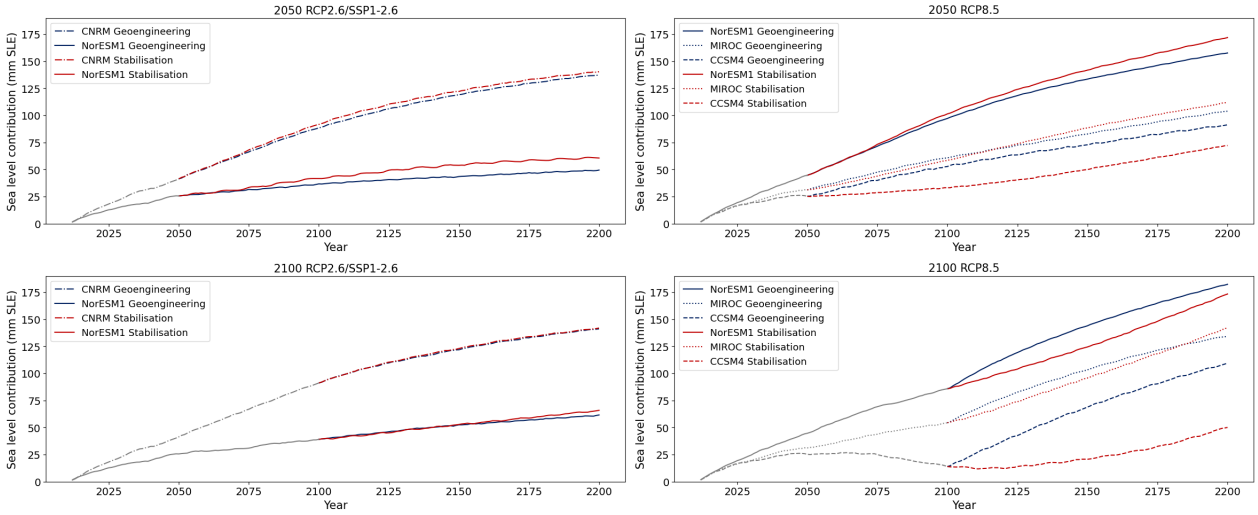

Figure 1. Total sea level contribution relative to 2012 shown in SLE (mm) for 2050 (top) and 2100 (bottom) for RCP2.6/SSP1-2.6 (left) and RCP8.5 (right) emission scenarios. Line types show different model experiments. *NorESM1*: solid line, *MIROC*: dotted line, *CCSM4*: dashed lined, *CNRM*: dash dotted line. Red lines indicate stabilisation scenarios, blue lines indicate geoengineering scenarios.

Figure 2a-d shows the G-S differences for SMB. Under low emissions, *CNRM 1-2.6* shows that geoengineering results in smaller SMB gains (negative G-S difference). In contrast, *NorESM1 2.6* has higher SMB under geoengineering for the 2050 scenario (positive G-S difference) and a negligible difference for the 2100 scenario. All show smaller G-S differences and the largest differences are between the models themselves.

All high emission simulations show smaller SMB gains under geoengineering than stabilisation. SMB gains and G-S differences are larger in the 2100 simulations. The 2100 scenarios also have a clearer distinction between geoengineering and stabilisation as there is no overlap between scenarios. *CCSM4 8.5* has the strongest SMB response, showing the largest gains for both the 2050 (991mm) and 2100 (1116mm) experiments under stabilisation, as well as the largest G-S differences (85mm and 156mm).

3.3 Ice Dynamics

Estimates of ice dynamics sea level contribution were calculated by subtracting the integrated SMB from the total sea level contribution, to better understand changes in Antarctic ice sheet volume not directly due to SMB. This calculation produces an ice dynamics contribution that can be attributed to both grounding line retreat and increased flux across across the grounding line.

Figure 2 (panels e-h) shows the G-S differences for ice dynamics. Under RCP2.6/SSP1-2.6, *NorESM1 2.6* has negligible G-S differences for both 2050 and 2100 scenarios. *CNRM 1-2.6* has G-S differences of 18mm and 14mm respectively, with geoengineering producing a smaller sea level contribution from ice dynamics than stabilisation. Both models have higher ice dynamics contributions for the 2100 experiments (Table B1).

Under RCP8.5, geoengineering results in smaller ice dynamics sea level contributions, whether implemented in 2050 or 2100, shown by the negative G-S differences. For the 2050 experiments, *CCSM4* has the largest G-S difference of 67mm, with *NorESM1*

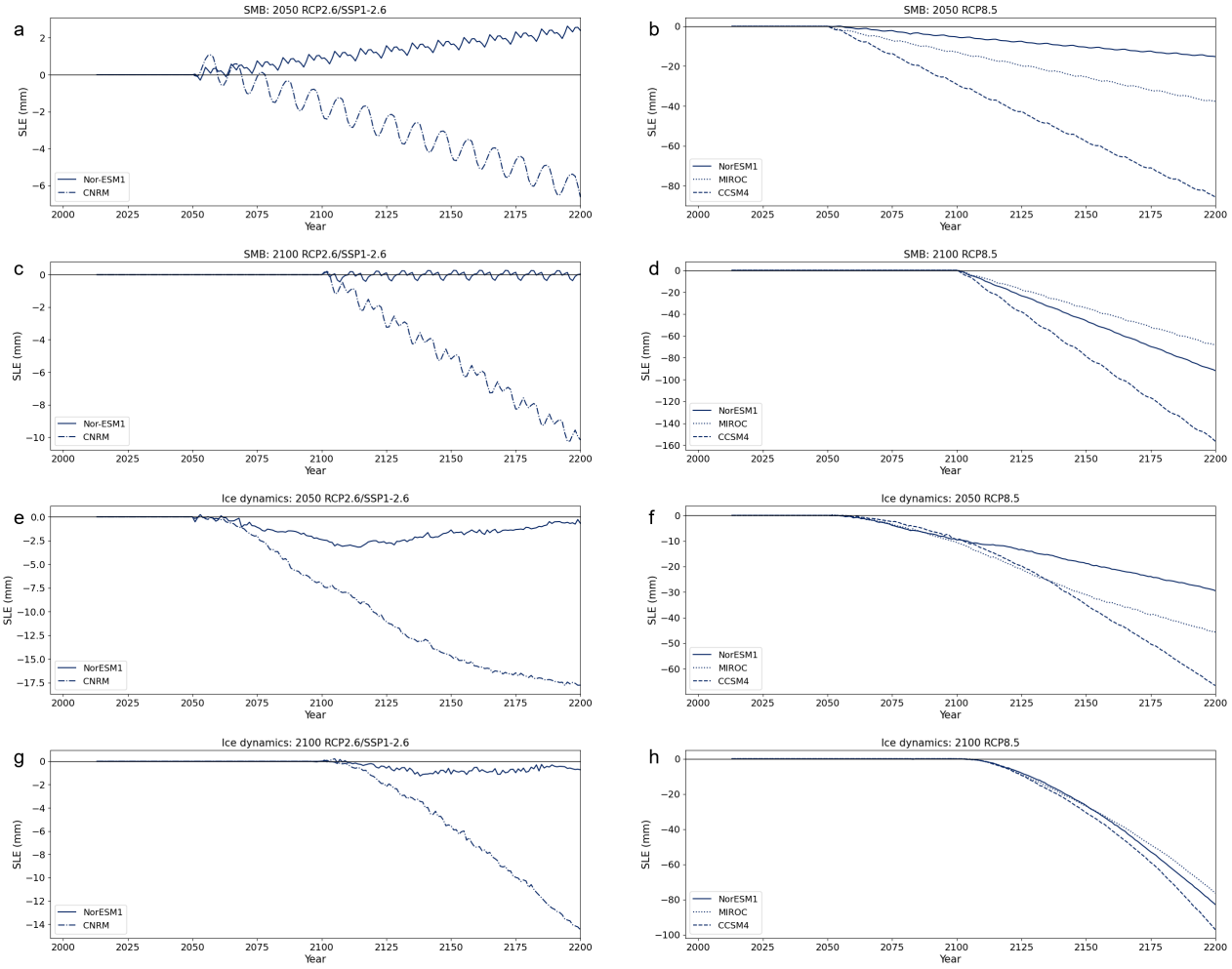

Figure 2. Difference between geoengineering and stabilisation scenarios (geoengineering minus stabilisation) for cumulative SMB (panels a-d) and ice dynamics (e-h). RCP2.6/SSP1-2.6 scenarios are shown in the left panels, and RCP8.5 scenarios are shown on the right. Line types show different model experiments. *NorESM1* – solid line, *MIROC* – dotted line, *CCSM4* – dashed lined, *CNRM* – dash dotted line. Positive (negative) values indicate that geoengineering has a larger (smaller) SMB or ice dynamics value than stabilisation.

having the smallest G-S difference of 30mm. For the 2100 experiments, the G-S difference is more pronounced for all models (76-97mm), and the ice dynamic sea level contribution is greater than compared with the 2050 experiments. G-S differences also appear to increase at an accelerating rate compared with the 2050 experiments' more linear response (with the exception of *CCSM4 8.5*). The acceleration in G-S difference is due to the sea level contribution from ice dynamics increasing at a faster rate under a stabilisation scenario than under geoengineering.

3.4 Spatial patterns of mass loss

Figure 3 presents spatial patterns of G-S differences for ice thickness. Geoengineering is helpful in reducing mass loss for the Amery and West ice Shelves, the Amundsen Sea Embayment, and Totten Glacier. The Ross and Ronne-Filchner ice shelves are more model dependent. All models show greater thickening in the interior under stabilisation compared with geoengineering. Though geoengineering does prevent some thinning, there are still large losses in these regions, under both geoengineering and stabilisation (B2)

Similar results are observed in the 2100 simulations, with losses observed in the same areas but with greater severity (Figure B3). The north coast of Queen Maud Land also experiences significant losses. The G-S difference is larger in the 2100 experiments (Figure 3), as is the inland thickening under stabilisation because of the increased SMB, and there is strong model agreement on geoengineering being beneficial to the Ross ice shelf.

Losses are smaller under RCP2.6/SSP1-2.6, but spatial patterns of thinning are similar (Figures B2 and B3). Though there is some thickening in the interior, G-S differences are much smaller for RCP2.6/SSP1-2.6 than under RCP8.5, indicating smaller SMB changes (Figure B4). All simulations demonstrate that geoengineering is less effective for the Ross ice shelf but is otherwise useful in many similar regions as the RCP8.5 experiments.

4 Discussion

All models agree that regardless of scenario, Antarctica will contribute considerably to sea level over the next two centuries. SMB plays an important role in driving changes across all scenarios, with ice dynamics also contributing significantly to the 2100 RCP8.5 emissions scenarios.

Scenarios with most warming show the largest SMB gains as warmer climates lead to increased precipitation. This is seen in the forcings (Figures A1 and A2), where for all models, the repeated decadal SMB forcing under stabilisation is higher than under geoengineering. This difference in climate forcing produces the large negative G-S differences for SMB seen for the RCP8.5 emissions scenarios, particularly for the 2100 simulations, indicating that geoengineering tends toward smaller SMB increases due to the reduced warming. For the 2100 RCP8.5 stabilisation scenarios, this increased SMB partially offsets some of the losses from Antarctica, resulting in smaller sea level contributions compared with geoengineering. This contrasts to what is seen in the 2050 RCP8.5 scenarios and all RCP2.6/SSP1-2.6 emission scenarios, as here the small forcing difference between geoengineering and stabilisation does not produce a SMB increase large enough to partially offset dynamic losses. *CCSM4 8.5* however, has a very large SMB increase, which is why this is the only 2050 experiment where sea level contribution under geoengineering is higher than under stabilisation: geoengineering dampens the SMB, while dynamic losses continue.

Though the 2100 RCP8.5 scenarios initially show larger sea level contributions under geoengineering, all geoengineering trajectories begin to slow, while the stabilisation trajectories accelerate (Figure 1), leading to the possibility of the scenarios eventually

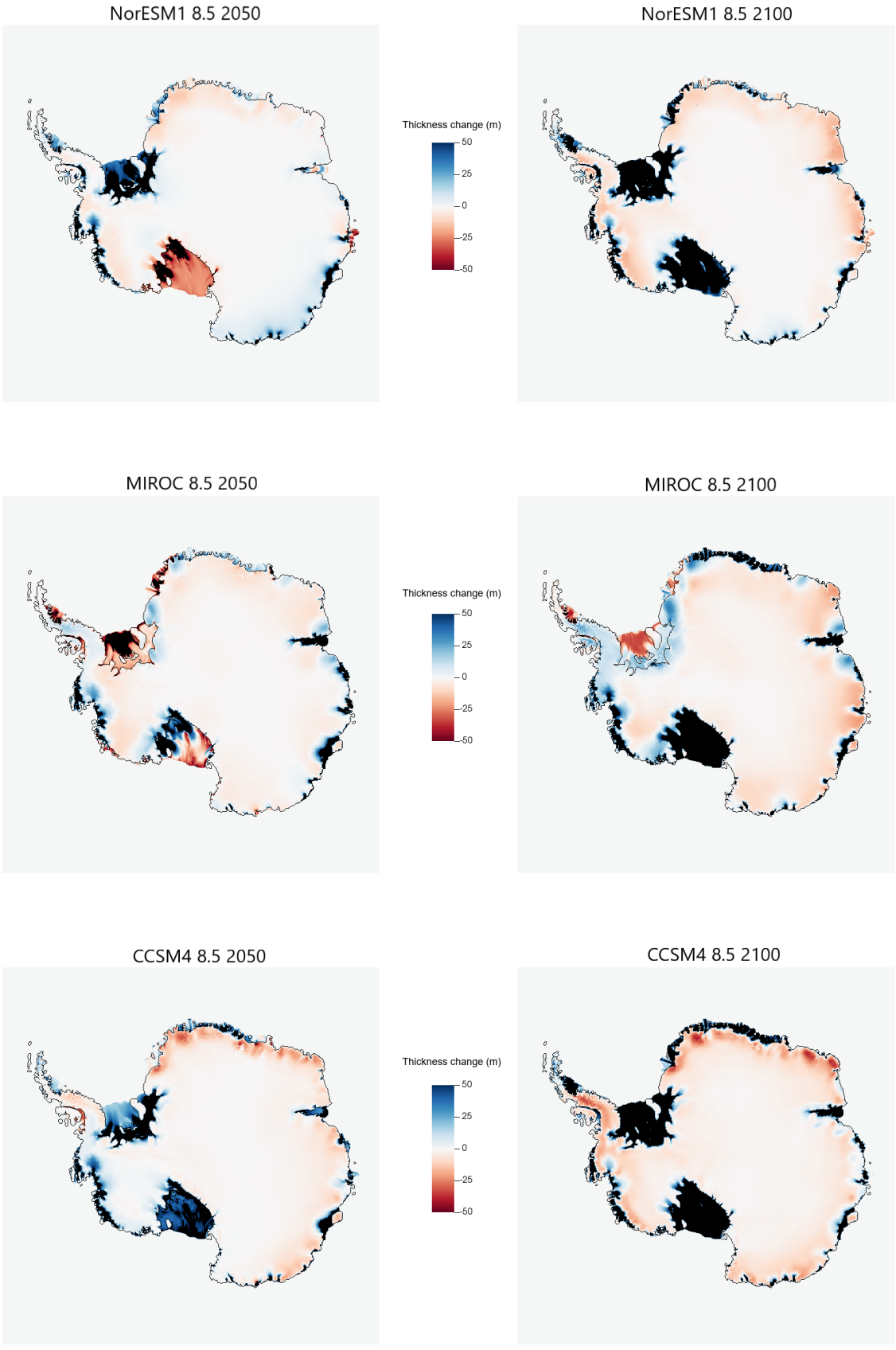

Figure 3. Spatial patterns of ice thickness difference in meters between geoengineering minus stabilisation for RCP8.5 experiments at 2200. 2050 experiments are shown on the left and 2100 shown on the right. Where values are negative (red), geoengineered ice thickness is less than the stabilisation experiments. Where values are positive (blue), geoengineered ice thickness is more than stabilisation experiments. Values higher than 50m or lower than -50m are shown in black.

converging. G-S differences peak and then decline (Figure B1), with *MIROC's* sea level contribution under stabilisation overtaking geoengineering in ∼2185 (Figure 1). Initially, increased SMB from warmer atmospheric temperatures in the stabilisation scenarios compensates for some of the losses: however, over time, the ice dynamic contribution increases substantially relative to the geoengineered scenarios. At this point, SMB increases are no longer enough to compensate for the dynamic losses. This has been found in previous work (Winkelmann et al., 2015; Golledge et al., 2015) and is seen here in Figure 2, where the 2100 RCP8.5 scenarios show an accelerating increase in G-S difference for ice dynamics, while the SMB G-S difference increases linearly.

The large rise in sea level contribution from ice dynamics under the high emission stabilisation scenarios is explained by the basal melt (Figure B5), which greatly increases compared to geoengineering. Figure 3, also shows thinner ice shelves under stabilisation, reducing buttressing and increasing ice flow. The G-S difference for the grounded area also accelerates because the grounded area under stabilisation continues to decrease, while it begins to plateau under geoengineering (Figure B6). All other scenarios show a stabilisation for both geoengineering and stabilisation. The 2100 RCP8.5 stabilisation scenarios could therefore point to a possible instability in grounding line retreat being triggered, which geoengineering could help to mitigate.

The Amery ice shelf, Totten and Amundsen Sea Embayment glaciers appear to be more unstable than others, as they continue to thin even when ocean thermal forcing reverts to present day under both low and high emissions scenarios. Observed rates of thinning and grounding line retreat are highest in the Amundsen and Bellingshausen Sea areas and around Totten Glacier, and several Amundsen Sea Embayment glaciers have been stated as being compatible with the onset of MISI, though this is still uncertain (IPCC, 2021, 2019)

The lagged response of the ice sheet to past warming means that geoengineering is unable to prevent mass loss, even in this idealised case where ocean forcing is instantly decreased. In reality, sea level contributions would likely be even higher as the additional ocean inertia would mean that ocean thermal forcing would remain at 2050 or 2100 levels for decades, even if atmospheric temperatures were immediately reduced. CDW, for example, is a relatively old (Matsumoto, 2007) and deep (Jacobs et al., 2011) water mass. This means it is not in frequent contact with the atmosphere, and that these deeper waters take time to adjust to atmospheric changes as they penetrate down from the surface. The ocean's lagged response time has been previously proposed as the reason Antarctica will have committed sea level rise, even if atmospheric temperatures were stabilised (DeConto et al., 2021).

The models show little agreement on sea level contribution, and high and low emission scenarios overlap between models in many cases. Figures A1 andA2 show that SMB and ocean thermal anomalies have large interannual variability, meaning these results depend strongly on the decade chosen to repeat. Particularly for the low emission scenarios, there is considerable overlap between stabilisation and geoengineering input forcings, which may explain why smaller changes are seen between the two, and why the largest differences are seen between models. The model and decade chosen therefore play a comparably large role in determining Antarctic sea level contribution. As these scenarios are highly idealized, we do not focus on projecting absolute sea level contribution. Instead, we focus on understanding whether geoengineering leads to more effective sea level rise mitigation than stabilising climate at 2050 or 2100. The simulations also provide insight into the reversibility of mass loss from Antarctica: that while idealised, large scale geoengineering can mitigate some loss, it cannot reverse it.

5 Conclusion

Although the Antarctic ice sheet will contribute substantially to sea level rise in all cases, implementing geoengineering in 2050 generally results in decreases in sea level contribution compared with stabilising the climate at 2050 or 2100. The climate model *CCSM4* under an RCP8.5 scenario is an exception, as its strong SMB response offsets some sea level contribution in the stabilisation scenario. If geoengineering methods are deployed in 2100, outcomes are more uncertain, and under high emission scenarios, geoengineering often initially contributes more to sea level rise than stabilising climate in 2100, due to increased SMB offsetting some of the mass loss. Beyond 2200, however, sea level contribution under stabilisation appears to accelerate, likely as a result of increased losses due to ice dynamics, whilst the geoengineering scenarios' sea level contribution decelerates. This could indicate that in future, geoengineering may eventually be more effective.

Sea level contributions differ widely between models for the same scenario, with this difference often being larger than the difference between the geoengineering and stabilisation scenarios. Under RCP8.5, models do not all agree that geoengineering in 2050 would be more effective than stabilising the climate. The model uncertainty therefore makes it difficult to quantify the effectiveness of geoengineering, however the results still highlight that Antarctic mass loss is irreversible for the next two centuries due to its delayed response to climate forcings.

More work is needed to understand Antarctica's response to more realistic geoengineered scenarios, but the results presented here indicate that geoengineering would not be a complete solution to mitigating sea level contribution from the ice sheet, nor reverse it on multi-century timescales. Deployment would be more effective if implemented earlier, and if delayed until the end of the century, would initially be more harmful than stabilising the climate. As substantial mass losses are still seen under a 2050 implementation, it is likely that even an earlier implementation of geoengineering would not be able to fully prevent further sea level contribution. Additional mitigation and adaptation strategies will therefore still need to be investigated.

6 Open research

We use BISICLES version 1.3, revision number 4311 of the public branch, accessible at `https://anag-repo.lbl.gov/svn/BISICLES/public/trunk/`. BISICLES is written in a combination of C++ and FORTRAN and is built upon the Chombo AMR software framework. More information about Chombo can be found at `http://Chombo.lbl.gov`.

ISMIP6 atmosphere and ocean forcing data is stored on the University of Buffalo's CCR transfer server, accessed at sftp://transfer.ccr.buffalo.edu/projects/grid/ghub/ISMIP6. Instructions for accessing the server can be found at: `https://www.climate-cryosphere.org/wiki/index.php?title=ISMIP6-Projections-Antarctica#A2.2_Retrieving_dataset_and_Uploading_your_model_output`

The data that support the findings of this study are openly available at `https://data.mendeley.com/preview/y3vg6c68th?a=d675fa69-5403-40ec-8422-96f347654d63`.

Figures were created using Matplotlib version 3.7 and Pandas version 1.5.3. Maps were creating using VisIt version 3.1.0, available at `https://sd.llnl.gov/simulation/computer-codes/visit/executables`

Appendix A Climate forcing inputs

Appendix A shows all input forcings used, illustrating the repeated decadal timeslices.

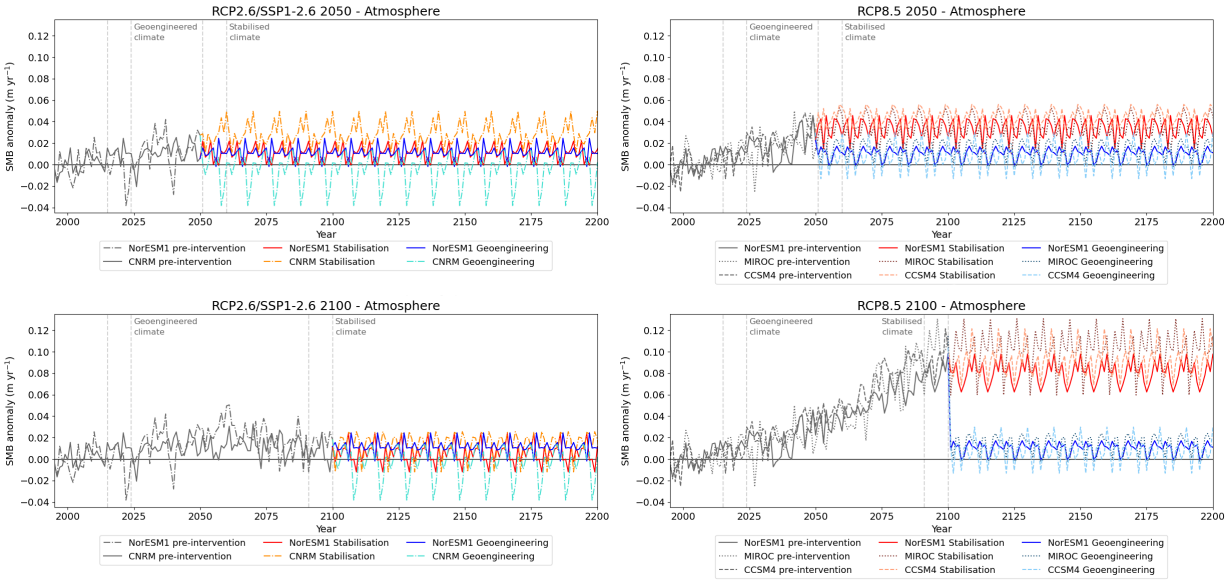

Figure A1. SMB anomalies for 2050 (top) and 2100 (bottom) for RCP2.6/SSP1-2.6 (left) and RCP8.5 (right) emission scenarios. Different line types show different model experiments. *NorESM1* – solid line, *MIROC* – dotted line, *CCSM4* – dashed lined, *CNRM* – dash dotted line. Red/orange lines indicate stabilisation scenarios, blue lines indicate geoengineering scenarios. The grey vertical dashed lines show the repeated time periods of geoengineered (2015-2024) and stabilisation (2051-2060/2091-2100) climates.

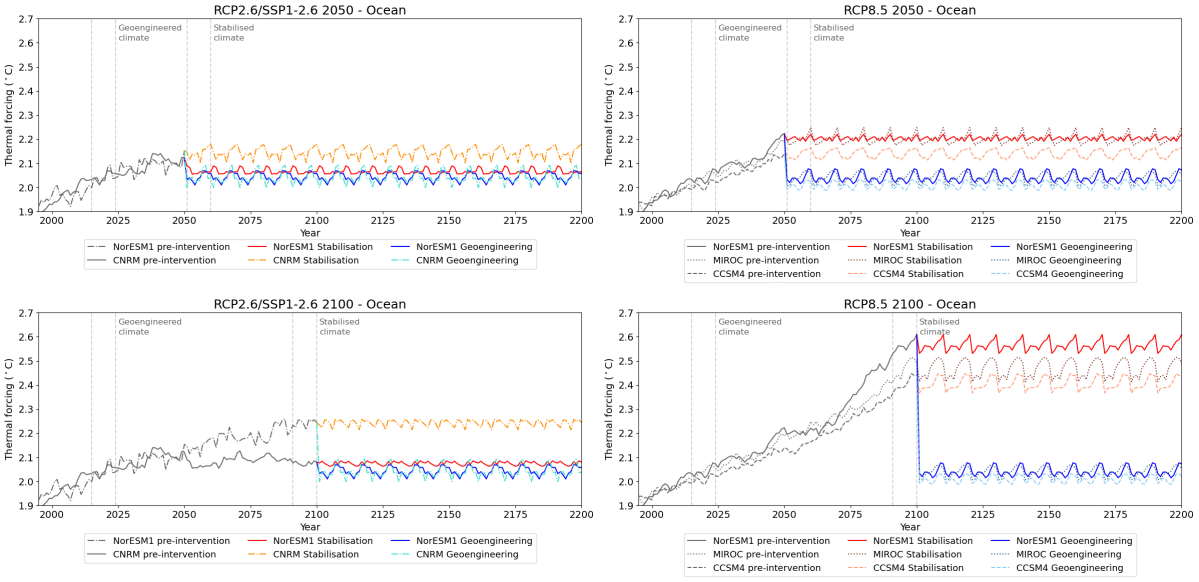

Figure A2. As A1 but for ocean thermal forcing.

Appendix B Further results and variables

Appendix B contains a table of all 2200 values relative to 2012 for total sea level contribution, SMB, ice dynamics, total melt, and grounded area change (Table B1). It contains timeseries showing the G-S difference for total sea level contribution (B1), absolute sea level contribution from melt (B5) and grounded area change (B6), and spatial patterns of mass loss (B2, B3 and B4).

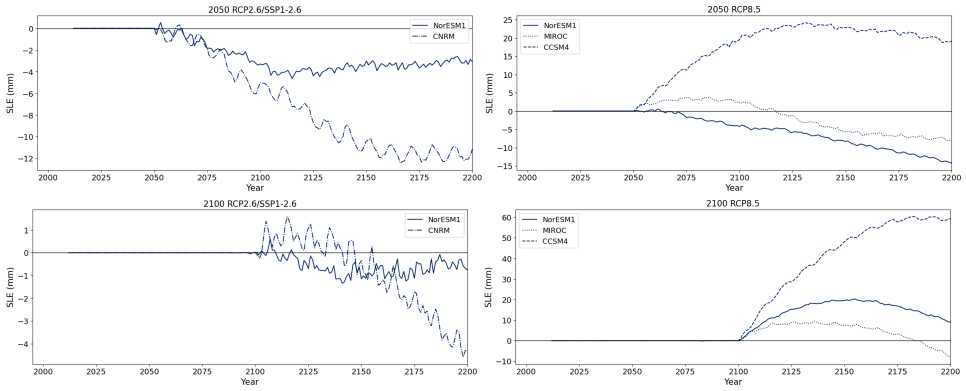

Figure B1. Difference between the geoengineering and stabilisation scenarios (geoengineering minus stabilisation) for total sea level contribution, for 2050 (top) and 2100 (bottom) for RCP2.6/SSP1-2.6 (left) and RCP8.5 (right) emission scenarios. Different line types show different model experiments. *NorESM1* – solid line, *MIROC* – dotted line, *CCSM4* – dashed lined, *CNRM* – dash dotted line. Where the value is positive, geoengineering has a larger sea level contribution than stabilisation, i.e. that geoengineering is worse than fixing the climate at that point. If the value is negative, then geoengineering has a smaller sea level contribution than stabilisation.

Acknowledgments

Financial support for this study was provided by the London NERC DTP (Refs NE/S007229/1 and NE/L002485/1) and through the Scientific Discovery through Advanced Computing (SciDAC) program funded by the U.S. Department of Energy (DOE), Office of Science, Biological and Environmental Research and Advanced Scientific Computing Research programs, as a part of the ProSPect SciDAC Partnership. Work at Berkeley Lab was supported by the Director, Office of Science, of the U.S. Department of Energy under Contract No. DE-AC02-05CH11231. This research used resources of the National Energy Research Scientific Computing Center (NERSC), a U.S. Department of Energy Office of Science User Facility located at Lawrence Berkeley National Laboratory, operated under Contract No. DE-AC02-05CH11231 using NERSC award ASCR-ERCAPm1041.

References

Barthel, A., Agosta, C., Little, C. M., Hattermann, T., Jourdain, N. C., Goelzer, H., ... Bracegirdle, T. J. (2020, March). CMIP5 model selection for ISMIP6 ice sheet model forcing: Greenland and Antarctica. *The Cryosphere*, *14*(3), 855–879. Retrieved from `https://tc.copernicus.org/articles/14/855/2020/` doi: 10.5194/tc-14-855-2020

Bulthuis, K., Arnst, M., Sun, S., & Pattyn, F. (2019, April). Uncertainty quantification of the multi-centennial response of the Antarctic ice sheet to cli-

Table B1. Projections in 2200 relative to 2012 for total sea level contribution, integrated SMB, integrated ice dynamics, integrated basal melt, and grounded area change, for all experiments, shown in mm sea level equivalent

	Stabilisation 2050	Geoengineering 2050	Stabilisation 2100	Geoengineering 2100
Total sea level contribution (SLE mm)				
NorESM1 8.5	171	157	172	181
MIROC 8.5	111	103	142	134
CCSM4 8.5	72	91	50	109
NorESM1 2.6	140	137	141	141
CNRM 1-2.6	60	49	65	61
SMB cumulative sum (SLE mm)				
NorESM1 8.5	-879	-859	-976	-885
MIROC 8.5	-946	-908	-997	-928
CCSM4 8.5	-991	-905	-1116	-959
NorESM1 2.6	-873	-875	-875	-875
CNRM 1-2.6	-966	-960	-974	-964
Ice dynamics cumulative sum (SLE mm)				
NorESM1 8.5	1051	1021	1154	1071
MIROC 8.5	1058	1012	1139	1063
CCSM4 8.5	1063	997	1166	1069
NorESM1 2.6	1013	1012	1017	1017
CNRM 1-2.6	1027	1009	1040	1025
Melt cumulative sum (SLE mm)				
NorESM1 8.5	358	253	926	466
MIROC 8.5	474	291	1267	504
CCSM4 8.5	424	211	981	390
NorESM1 2.6	153	184	180	191
CNRM 1-2.6	284	314	366	335
Grounded area change (km^2/1000)				
NorESM1 8.5	-215	-186	-302	-234
MIROC 8.5	-217	-188	-293	-227
CCSM4 8.5	-222	-171	-319	-226
NorESM1 2.6	-150	-170	-156	-168
CNRM 1-2.6	-148	-180	-162	-176

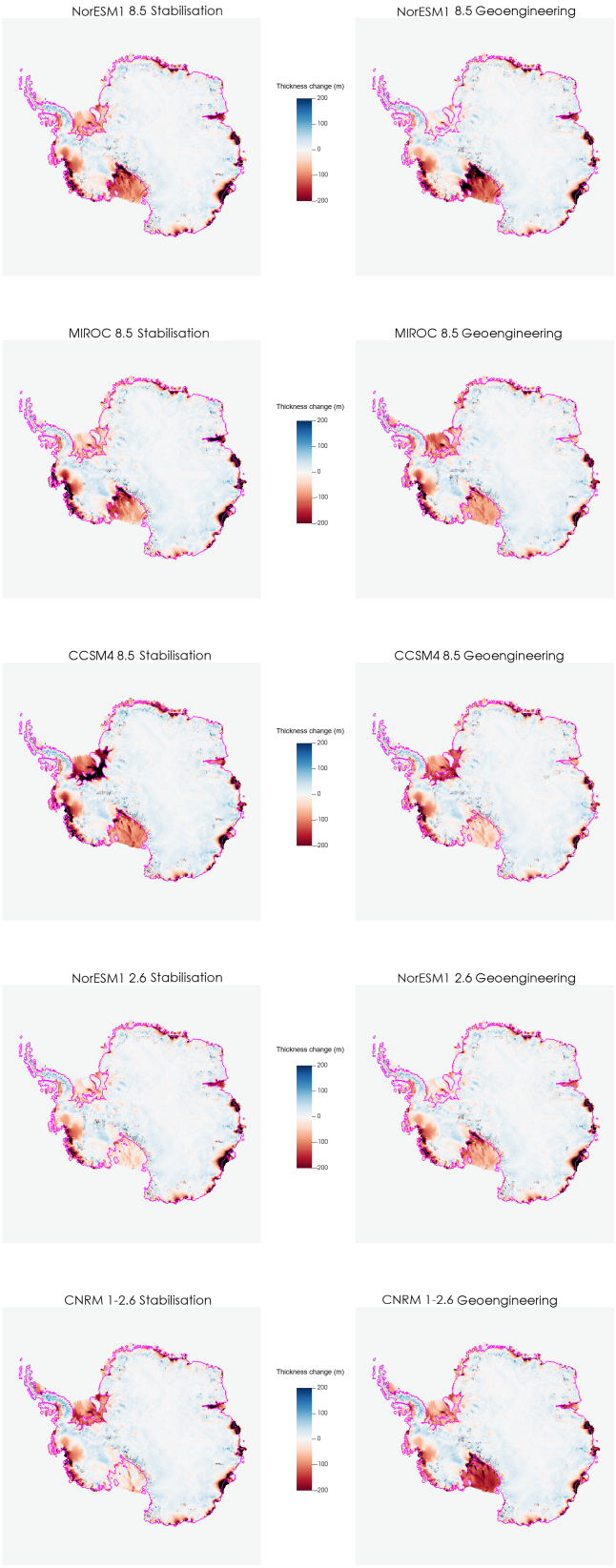

Figure B2. Thickness change in meters between 2012 and 2200 for the 2050 experiments. Pink line denotes the grounding line. Red areas represent areas where ice thickness is lower in 2200 compared with 2012. Values higher than 200m or lower than -200m are shown in black.

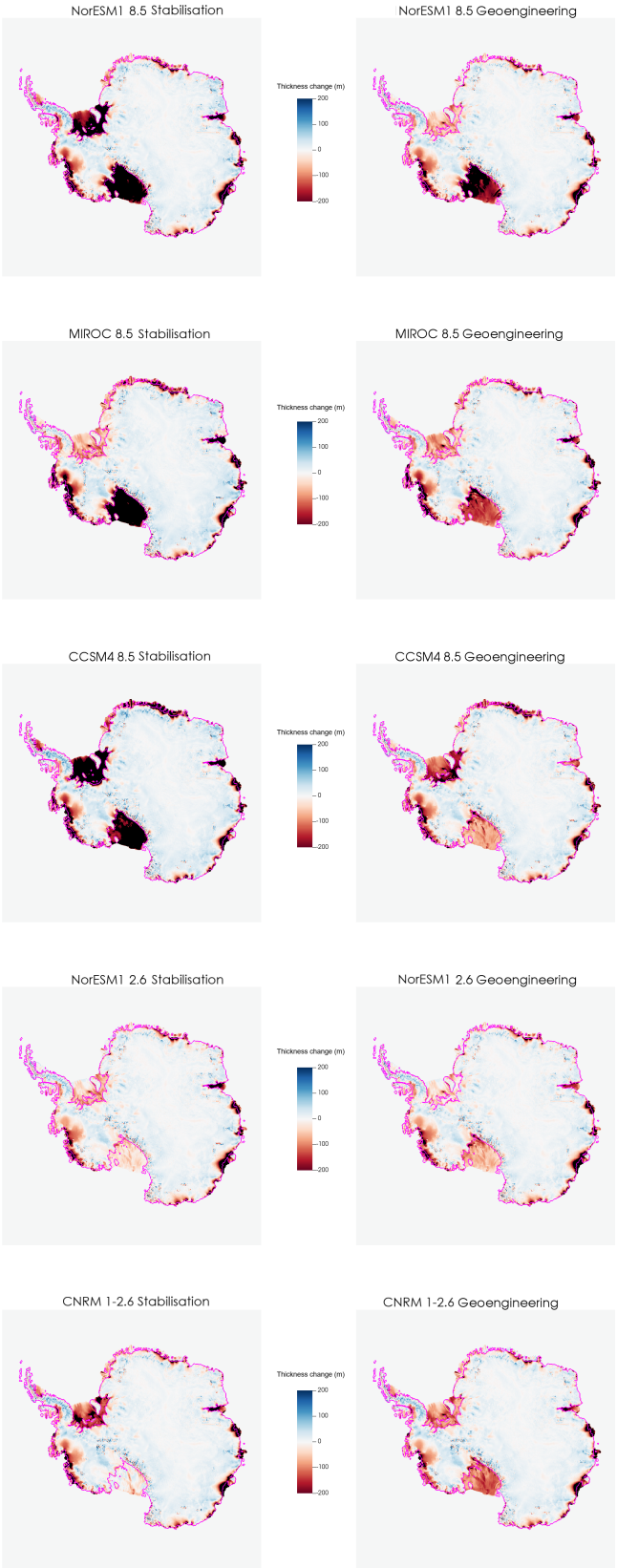

Figure B3. As B2 but for the 2100 scenarios.

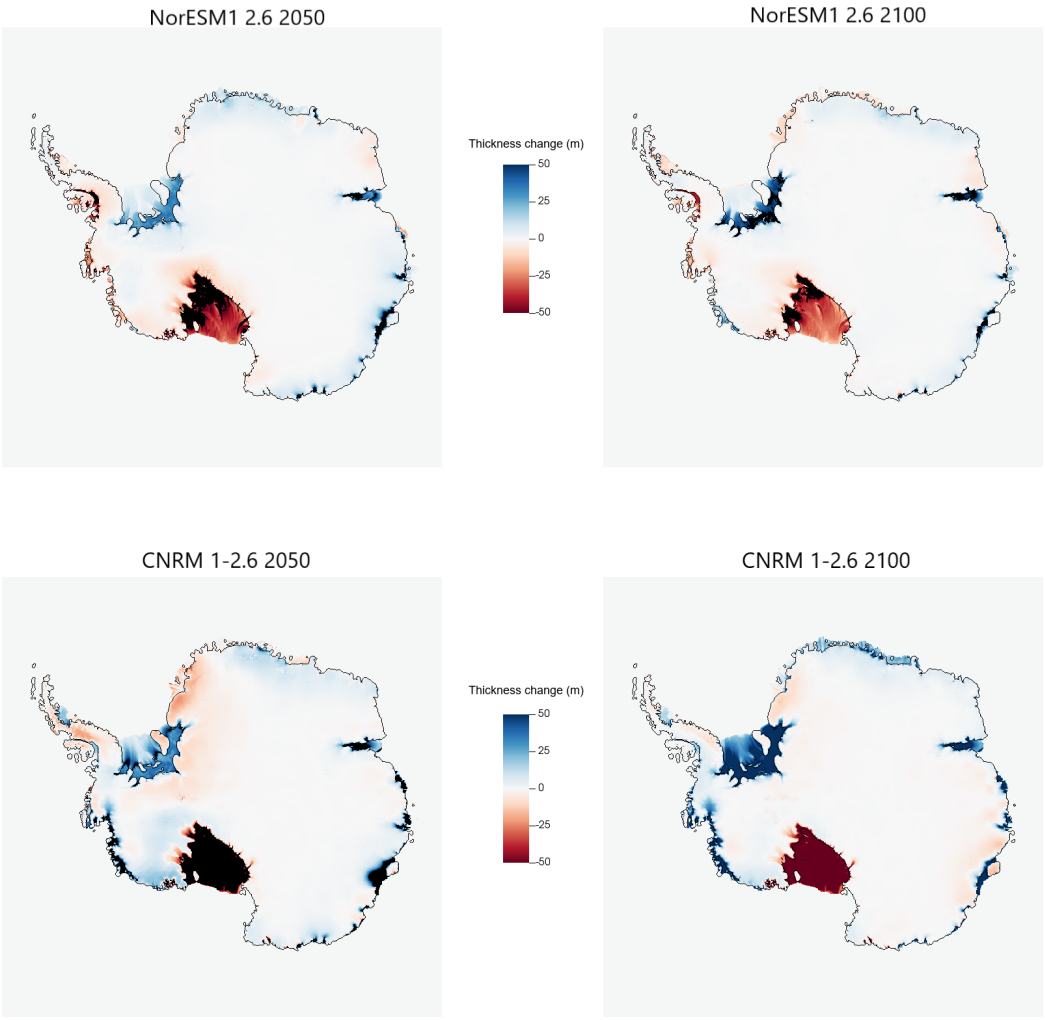

Figure B4. Spatial patterns of ice thickness difference between geoengineering minus stabilisation for RCP2.6/SSP1-2.6 experiments at 2200. Thickness difference shown in meters. 2050 experiments are shown on the left and 2100 shown on the right. Where values are negative (red), geoengineered ice thickness is less than the stabilisation experiments. Where values are positive (blue), geoengineered ice thickness is more than stabilisation experiments. Values higher than 50m or lower than -50m are shown in black.

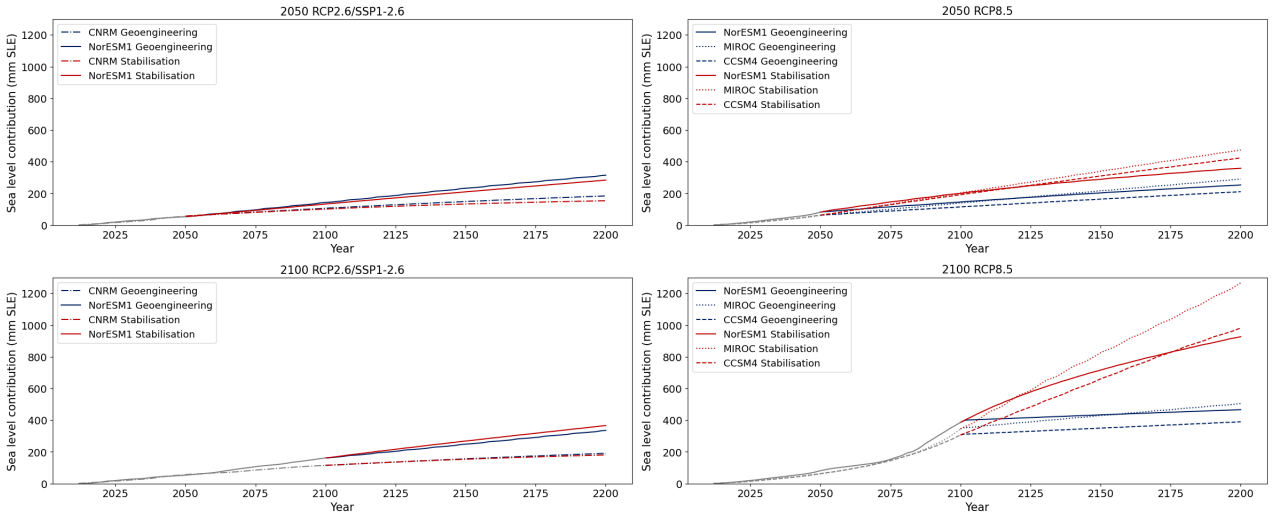

Figure B5. Cumulative sum of total melt relative to 2012 shown in SLE for 2050 (top) and 2100 (bottom) for RCP2.6/SSP1-2.6 (left) and RCP8.5 (right) emission scenarios. Different line types show different model experiments. *NorESM1* – solid line, *MIROC* - dotted line, *CCSM4* - dashed lined, *CNRM* - dash dotted line. Red lines indicate stabilisation scenarios, blue lines indicate geoengineering scenarios.

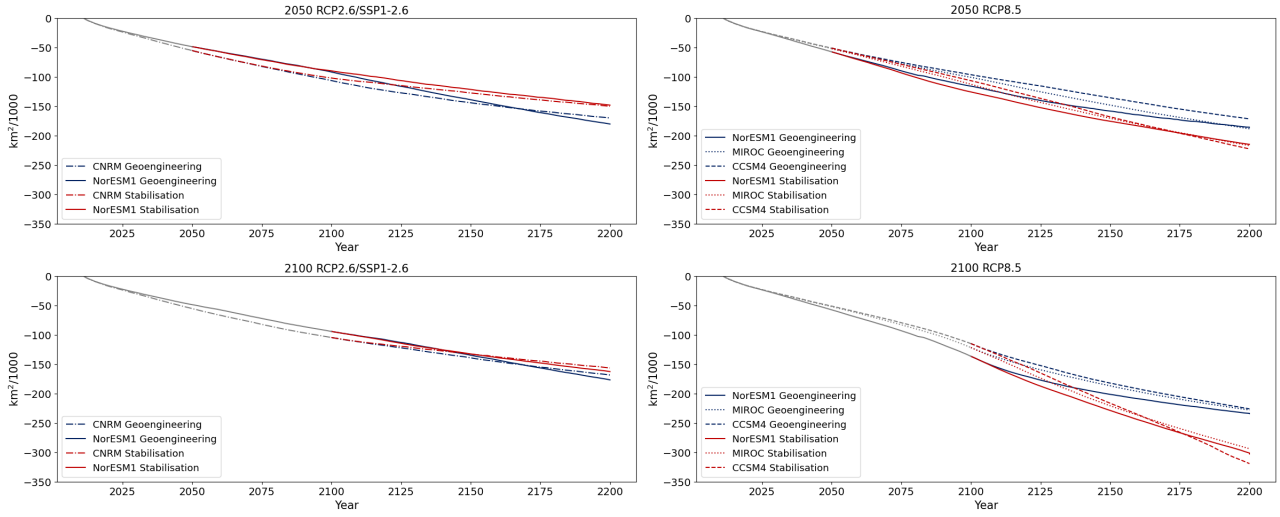

Figure B6. Grounded area change relative to 2012 for 2050 (top) and 2100 (bottom) for RCP2.6/SSP1-2.6 (left) and RCP8.5 (right) emission scenarios. Different line types show different model experiments. *NorESM1* – solid line, *MIROC* - dotted line, *CCSM4* - dashed lined, *CNRM* - dash dotted line. Red lines indicate stabilisation scenarios, blue lines indicate geoengineering scenarios.

mate change. *The Cryosphere*, *13*(4), 1349–1380. Retrieved 2022-02-26, from https://tc.copernicus.org/articles/13/1349/2019/ doi: 10.5194/tc-13-1349-2019

Cornford, S. L., Martin, D. F., Graves, D. T., Ranken, D. F., Le Brocq, A. M., Gladstone, R. M., ... Lipscomb, W. H. (2013, January). Adaptive mesh, finite volume modeling of marine ice sheets. *Journal of Computational Physics*, *232*(1), 529–549. Retrieved 2021-02-08, from https://linkinghub.elsevier.com/retrieve/pii/S0021999112005050 doi: 10.1016/j.jcp.2012.08.037

DeConto, R. M., & Pollard, D. (2016, March). Contribution of Antarctica to past and future sea-level rise. *Nature*, *531*(7596), 591–597. Retrieved 2021-02-11, from http://www.nature.com/articles/nature17145 doi: 10.1038/nature17145

DeConto, R. M., Pollard, D., Alley, R. B., Velicogna, I., Gasson, E., Gomez, N., ... Dutton, A. (2021, May). The Paris Climate Agreement and future sea-level rise from Antarctica. *Nature*, *593*(7857), 83–89. Retrieved 2022-02-26, from http://www.nature.com/articles/s41586-021-03427-0 doi: 10.1038/s41586-021-03427-0

Edwards, T. L., Nowicki, S., Marzeion, B., Hock, R., Goelzer, H., Seroussi, H., ... Zwinger, T. (2021, May). Projected land ice contributions to twenty-first-century sea level rise. *Nature*, *593*(7857), 74–82. Retrieved 2022-02-23, from http://www.nature.com/articles/s41586-021-03302-y doi: 10.1038/s41586-021-03302-y

Garbe, J., Albrecht, T., Levermann, A., Donges, J. F., & Winkelmann, R. (2020, September). The hysteresis of the Antarctic Ice Sheet. *Nature*, *585*(7826), 538–544. Retrieved 2021-03-02, from http://www.nature.com/articles/s41586-020-2727-5 doi: 10.1038/s41586-020-2727-5

Golledge, N. R., Kowalewski, D. E., Naish, T. R., Levy, R. H., Fogwill, C. J., & Gasson, E. G. W. (2015, October). The multi-millennial Antarctic commitment to future sea-level rise. *Nature*, *526*(7573), 421–425. Retrieved 2022-03-03, from http://www.nature.com/articles/nature15706 doi: 10.1038/nature15706

Gudmundsson, G. H. (2013, April). Ice-shelf buttressing and the stability of marine ice sheets. *The Cryosphere*, *7*(2), 647–655. Retrieved 2021-02-10, from https://tc.copernicus.org/articles/7/647/2013/ doi: 10.5194/tc-7-647-2013

Hanna, E., Navarro, F. J., Pattyn, F., Domingues, C. M., Fettweis, X., Ivins, E. R., ... Zwally, H. J. (2013, June). Ice-sheet mass balance and climate change. *Nature*, *498*(7452), 51–59. Retrieved 2023-09-26, from https://www.nature.com/articles/nature12238 doi: 10.1038/nature12238

IPCC. (2019). *The Ocean and Cryosphere in a Changing Climate: Special Report of the Intergovernmental Panel on Climate Change* (1st ed.). Cambridge University Press. Retrieved 2023-04-28, from https://www.cambridge.org/core/product/identifier/9781009157964/type/book doi: 10.1017/9781009157964

IPCC. (2021). *IPCC, 2021: Climate Change 2021: The Physical Science Basis. Contribution of Working Group I to the Sixth Assessment Report of the Intergovernmental Panel on Climate Change* (Tech. Rep.). Cambridge University Press.

Irvine, P. J., Keith, D. W., & Moore, J. (2018, July). Brief communication: Understanding solar geoengineering's potential to limit sea level rise requires attention from cryosphere experts. *The Cryosphere*, *12*(7), 2501–2513. Retrieved 2021-01-21, from https://tc.copernicus.org/articles/12/2501/2018/ doi: 10.5194/tc-12-2501-2018

Jacobs, S. S., Jenkins, A., Giulivi, C. F., & Dutrieux, P. (2011, August). Stronger ocean circulation and increased melting under Pine Island Glacier ice

shelf. *Nature Geoscience*, *4*(8), 519–523. Retrieved 2021-02-03, from http://www.nature.com/articles/ngeo1188 doi: 10.1038/ngeo1188

Jourdain, N. C., Asay-Davis, X., Hattermann, T., Straneo, F., Seroussi, H., Little, C. M., & Nowicki, S. (2020, September). A protocol for calculating basal melt rates in the ISMIP6 Antarctic ice sheet projections. *The Cryosphere*, *14*(9), 3111–3134. Retrieved 2021-03-02, from https://tc.copernicus.org/articles/14/3111/2020/ doi: 10.5194/tc-14-3111-2020

Kittel, C., Amory, C., Agosta, C., Jourdain, N. C., Hofer, S., Delhasse, A., ... Fettweis, X. (2020, October). *Diverging future surface mass balance between the Antarctic ice shelves and grounded ice sheet* (preprint). Ice sheets/Antarctic. Retrieved 2023-09-27, from https://tc.copernicus.org/preprints/tc-2020-291/tc-2020-291.pdf doi: 10.5194/tc-2020-291

Lockley, A., Wolovick, M., Keefer, B., Gladstone, R., Zhao, L.-Y., & Moore, J. C. (2020, December). Glacier geoengineering to address sea-level rise: A geotechnical approach. *Advances in Climate Change Research*, S1674927820300940. Retrieved 2021-01-21, from https://linkinghub.elsevier.com/retrieve/pii/S1674927820300940 doi: 10.1016/j.accre.2020.11.008

Lowry, D. P., Krapp, M., Golledge, N. R., & Alevropoulos-Borrill, A. (2021, December). The influence of emissions scenarios on future Antarctic ice loss is unlikely to emerge this century. *Communications Earth & Environment*, *2*(1), 221. Retrieved 2021-10-25, from https://www.nature.com/articles/s43247-021-00289-2 doi: 10.1038/s43247-021-00289-2

Matsumoto, K. (2007, September). Radiocarbon-based circulation age of the world oceans. *Journal of Geophysical Research: Oceans*, *112*(C9), 2007JC004095. Retrieved 2023-10-12, from https://agupubs.onlinelibrary.wiley.com/doi/10.1029/2007JC004095 doi: 10.1029/2007JC004095

Morlighem, M., Rignot, E., Binder, T., Blankenship, D., Drews, R., Eagles, G., ... Young, D. A. (2020). Deep glacial troughs and stabilizing ridges unveiled beneath the margins of the Antarctic ice sheet. *Nature Geoscience*, *13*(2), 132–137. Retrieved from https://doi.org/10.1038/s41561-019-0510-8 doi: 10.1038/s41561-019-0510-8

Nowicki, S., Payne, A., Larour, E., Seroussi, H., Goelzer, H., Lipscomb, W., ... Shepherd, A. (2016, December). Ice Sheet Model Intercomparison Project (ISMIP6) contribution to CMIP6. *Geoscientific Model Development*, *9*(12), 4521–4545. Retrieved 2021-02-28, from https://gmd.copernicus.org/articles/9/4521/2016/ doi: 10.5194/gmd-9-4521-2016

O'Neill, J., Edwards, T., Martin, D. F., Schafer, C., Cornford, S. L., Adhikari, M., ... Seroussi, H. (2024). ISMIP6 Antarctic Projections with the BISICLES ice sheet model to 2100 (preprint). *The Cryosphere Discussions*.

O'Neill, J. F., Edwards, T. L., Martin, D. F., Shafer, C., Cornford, S. L., Seroussi, H. L., ... Adhikari, M. (2024, February). *ISMIP6-based Antarctic Projections to 2100: simulations with the BISICLES ice sheet model* (preprint). Ice sheets/Antarctic. Retrieved 2024-03-13, from https://egusphere.copernicus.org/preprints/2024/egusphere-2024-441/ doi: 10.5194/egusphere-2024-441

Pattyn, F., & Morlighem, M. (2020, March). The uncertain future of the Antarctic Ice Sheet. *Science*, *367*(6484), 1331–1335. Retrieved 2021-02-01, from https://www.sciencemag.org/lookup/doi/10.1126/science.aaz5487 doi: 10.1126/science.aaz5487

Payne, A. J., Nowicki, S., Abe-Ouchi, A., Agosta, C., Alexander, P., Albrecht, T., ... Zwinger, T. (2021, August). Future Sea Level Change Under Coupled Model Intercomparison Project Phase 5 and Phase 6 Scenarios From the Greenland and Antarctic Ice Sheets. *Geophysical Research Letters*, *48*(16), e2020GL091741. Retrieved 2023-09-27, from https://agupubs.onlinelibrary.wiley.com/doi/10.1029/2020GL091741 doi:

10.1029/2020GL091741

Pritchard, H. D., Ligtenberg, S. R. M., Fricker, H. A., Vaughan, D. G., van den Broeke, M. R., & Padman, L. (2012, April). Antarctic ice-sheet loss driven by basal melting of ice shelves. *Nature*, *484*(7395), 502–505. Retrieved 2021-02-03, from http://www.nature.com/articles/nature10968 doi: 10.1038/nature10968

Rignot, E., & Jacobs, S. (2002, June). Rapid Bottom Melting Widespread near Antarctic Ice Sheet Grounding Lines. *Science*, *296*(5575), 2020–2023. Retrieved 2021-02-01, from https://www.sciencemag.org/lookup/doi/10.1126/science.1070942 doi: 10.1126/science.1070942

Schoof, C. (2007, July). Ice sheet grounding line dynamics: Steady states, stability, and hysteresis. *Journal of Geophysical Research*, *112*(F3), F03S28. Retrieved 2021-02-01, from http://doi.wiley.com/10.1029/2006JF000664 doi: 10.1029/2006JF000664

Seroussi, H., Nowicki, S., Simon, E., Abe-Ouchi, A., Albrecht, T., Brondex, J., ... Zhang, T. (2019, May). initMIP-Antarctica: an ice sheet model initialization experiment of ISMIP6. *The Cryosphere*, *13*(5), 1441–1471. Retrieved 2021-03-02, from https://tc.copernicus.org/articles/13/1441/2019/ doi: 10.5194/tc-13-1441-2019

Sutter, J., Jones, A., Frölicher, T. L., Wirths, C., & Stocker, T. F. (2023, September). Climate intervention on a high-emissions pathway could delay but not prevent West Antarctic Ice Sheet demise. *Nature Climate Change*, *13*(9), 951–960. Retrieved 2024-01-11, from https://www.nature.com/articles/s41558-023-01738-w doi: 10.1038/s41558-023-01738-w

Weertman, J. (1974). Stability of the Junction of an Ice Sheet and an Ice Shelf. *Journal of Glaciology*, *13*(67), 3–11. Retrieved 2021-01-21, from https://www.cambridge.org/core/product/identifier/S0022143000023327/type/journal_article doi: 10.3189/S0022143000023327

Winkelmann, R., Levermann, A., Ridgwell, A., & Caldeira, K. (2015). Combustion of available fossil fuel resources sufficient to eliminate the Antarctic Ice Sheet. *Science Advances*, *1*(8), e1500589. Retrieved from https://www.science.org/doi/abs/10.1126/sciadv.1500589 doi: 10.1126/sciadv.1500589